Modulation of Curli Assembly and Pellicle Biofilm Formation by Chemical and Protein Chaperones

Emma K. Andersson[1,2], **Christoffer Bengtsson**[1,2], **Margery L. Evans**[3], **Erik Chorell**[1,2], **Magnus Sellstedt**[1,2], **Anders E.G. Lindgren**[2], **David A. Hufnagel**[3], **Moumita Bhattacharya**[4], **Peter M. Tessier**[4], **Pernilla Wittung-Stafshede**[2], **Fredrik Almqvist**[1,2,*], and **Matthew R. Chapman**[1,3,*]

[1]Umeå Centre for Microbial Research, Umeå University, 901 87 Umeå, Sweden

[2]Department of Chemistry, Umeå University, 901 87 Umeå, Sweden

[3]Department of Molecular, Cellular and Developmental Biology, University of Michigan, Ann Arbor, MI 48109-1048, USA

[4]Center for Biotechnology and Interdisciplinary Studies, Department of Chemical and Biological Engineering, Rensselaer Polytechnic Institute, Troy, NY 12180, USA

SUMMARY

Enteric bacteria assemble functional amyloid fibers, curli, on their surfaces that share structural and biochemical properties with disease-associated amyloids. Here, we test rationally designed 2-pyridone compounds for their ability to alter amyloid formation of the major curli subunit CsgA. We identified several compounds that discourage CsgA amyloid formation and several compounds that accelerate CsgA amyloid formation. The ability of inhibitor compounds to stop growing CsgA fibers was compared to the same property of the CsgA chaperone, CsgE. CsgE blocked CsgA amyloid assembly and arrested polymerization when added to actively polymerizing fibers. Additionally, CsgE and the 2-pyridone inhibitors prevented biofilm formation by *Escherichia coli* at the air-liquid interface of a static culture. We demonstrate that curli amyloid assembly and curli-dependent biofilm formation can be modulated not only by protein chaperones, but also by "chemical chaperones."

INTRODUCTION

Amyloid proteins are commonly associated with neurodegenerative disorders such as Alzheimer's disease, Huntington's disease, and Parkinson's disease (Chiti and Dobson, 2006). Seemingly unrelated proteins of various size and primary amino acid sequences can assemble into amyloids that share the same biophysical properties: amyloids are 4–12 nm wide fibers, have a cross β sheet structure, are highly resistant to denaturation, and bind

---

SUPPLEMENTAL INFORMATION

Supplemental Information includes Supplemental Experimental Procedures, two figures, and two tables and can be found with this article online at http://dx.doi.org/10.1016/j.chembiol.2013.07.017.

amyloid-specific dyes such as Congo red and thioflavin T (ThT) (Ban et al., 2003; Chapman et al., 2002). A growing number of "functional" amyloids can be assembled by many cell types to fulfill normal physiological processes, including regulation of melanin synthesis, information transfer, or as structural materials (Blanco et al., 2012; Fowler et al., 2006; Hammer et al., 2008).

Amyloids are commonly found as a protein component of the extracellular matrix in bacterial biofilms. Bacteria within the bio-film are protected from environmental strain, including disinfectants and antibiotics, causing biofilms to be a major concern in hospital and industrial settings. One of the best-studied functional amyloids is curli, an extracellular fiber produced by *Escherichia coli* and *Salmonella* species. Curli fibers are important for adhesion to inert surfaces as well as host cells, biofilm formation, and other community behaviors (Barnhart and Chapman, 2006). Rugose bacterial colony biofilms, or red, dry, and rough (rdar), develop on solid surfaces under conditions of low osmolarity and low temperature (Römling, 2005). Rdar communities have spatially distinct populations, as curliated bacteria are limited to the biofilm-air interface where they contribute to resistance to hydrogen peroxide and desiccation (DePas et al., 2013; White et al., 2006). *E. coli* can also establish curli-dependent biofilms, called pellicles, at liquid-air interface of static cultures (Cegelski et al., 2009).

Curli biogenesis is a highly regulated process and requires the products of two divergently transcribed operons (*csgBAC* and *csgDEFG*) (Hammar et al., 1995). The major subunit protein of curli is CsgA. CsgA is secreted to the cell surface as an unstructured protein and then templated into amyloid fibers by the minor curli subunit CsgB (Bian and Normark, 1997; Hammar et al., 1996, 2007, 2008; Shu et al., 2012; Wang et al., 2008). The amyloid core of CsgA consists of five imperfect repeating units (R1–R5). R1 and R5 are highly amyloidogenic, whereas R2, R3, and R4 contain gatekeeper residues that reduce their ability to form amyloids (Shewmaker et al., 2009; Wang et al., 2007, 2010). The secretion of CsgA and CsgB is dependent on CsgG, which forms an oligomeric pore in the outer membrane (Loferer et al., 1997; Robinson et al., 2006). CsgC is believed to function cooperatively with CsgG, although CsgC is dispensable for curli biogenesis and its function remains unknown (Taylor et al., 2011). The chaperone-like CsgF assists the CsgB-CsgA interaction and aids the nucleation of CsgA polymerization in vivo (Nenninger et al., 2009). CsgE is a putative chaperone of CsgA that also functions as a specificity factor in the periplasm to facilitate efficient curli subunit secretion (Nenninger et al., 2011; Robinson et al., 2006).

The use of functional amyloids as model systems to identify general amyloid inhibitors has recently generated several promising leads (Andersson and Chapman, 2013; Cegelski et al., 2009; Horvath et al., 2012; Romero et al., 2013). By screening for inhibition of curli amyloid formation, a ring-fused 2-pyridone molecule called FN075 (compound **1**) was identified as having potent antiamyloid activities (Table 1; Figure 1) (Cegelski et al., 2009). FN075 belongs to a class of 2-pyridones that was originally designed to mimic a C-terminal small peptide with several positions in the central fragment available for substitutions (positions 2, 6, 7, and 8; Figure 1). The rigidity in the bicyclic scaffold ensures that the 2-pyridones maintain a straight, peptide-like conformation that mimics an extended beta strand (Cegelski et al., 2009; Chorell et al., 2012). We have previously shown that the

peptidomimetic ring-fused 2-pyridone FN075 (compound **1**, Table 1; Figure 1) exerts a potent inhibitory effect on CsgA amyloid formation by stabilizing an off-pathway oligomeric form of the protein (Cegelski et al., 2009; Horvath et al., 2012).

In this work, we prepared a diverse library of substituted ring-fused 2-pyridones where we varied the substitution pattern on the central fragment to gain further structure activity relationships (Figure 1). In addition, we also designed close analogs of the known curli inhibitor, FN075 (herein referred to as "compound **1**") showing that small changes in the molecule have drastic consequences for the effect on CsgA polymerization. We also present small compounds that promote the formation of curli. Moreover, we have found that the putative chaperone CsgE is capable of not only preventing CsgA polymerization but also preventing biofilm formation and arresting polymerization of actively elongating fibers.

RESULTS

Compound Library and Initial Structure-Activity Relationships

To further study structure-activity relationships between CsgA and 2-pyridones, we initially tested a library of 65 compounds (Table 1; Table S1 available online) with various substitution patterns (varying positions 2, 6, 7, and 8 in Figure 1) for their ability to inhibit CsgA polymerization. The compounds were tested in vitro for their ability to modulate CsgA polymerization using the ThT assay (Table 1; Table S1). Without compound, CsgA aggregation into amyloid can be observed as a sigmoidal rise with distinguishable lag, growth, and stationary phases in ThT fluorescence as amyloid fibers are assembled (Naiki et al., 1989; Wang et al., 2007). None of the 65 compounds from the initial library resulted in increased inhibition of CsgA polymerization as compared to compound **1**, but several showed equivalent activity (Table 1).

Because compound **1** had the best ability to inhibit CsgA amyloid formation, we synthesized additional compounds (~40) using compound **1** as a starting point (Figure 1). Eight compounds were synthesized with changes to the central fragment of compound **1**. The modifications we made to compound **1** included: extending the peptidomimetic backbone by introducing an amine (compound **7**, Figure 1), adding rigidifying tricyclic structures (compound **8**, Figure 1), exchanging the five-membered thiazolino group with a six-membered sultam group (compounds **9** and **10**, Figure 1), making a desulfurized ring-opened analog (compound **11**, Figure 1), and oxidizing the sulfur to sulfoxide or sulfone (compounds **12** and **13**, Figure 1) (Horvath et al., 2013; Sellstedt and Almqvist, 2008). Compound **14** (Horvath et al., 2013) has both the extended peptidomimetic backbone and oxidized sulfur (Figure 1) (Sellstedt and Almqvist, 2009; Horvath et al., 2013; Berg et al., 2006). Finally, an additional three "control" compounds were synthesized to assess the importance of position 3, 7, and 8 (Figure 1) Compound **3** lacks the trifluoro group at position 8 (Sellstedt and Almqvist, 2009), compound **5** lacks the carboxylic acid at position 3, and compound **6** is missing the naphtyl group at position 7 (Table 1).

We also introduced acetylenes as a linker moiety at position 8 to see if compound activity would change with the 8-substituent farther away from the central fragment. In addition, the acetylenes allowed us to expand the library further to synthesize substituted triazoles at

position 8. The synthesis of these compounds was accomplished via copper (I) catalyzed azide alkyne cycloadditions (CuAAC), which gave 24 additional compounds (Table S2). The acetylene-substituted analogs were accessible via a regioselective Sonogashira coupling to the iodo-bromo-substituted analog **15** (Figure 2). This resulted in the R^3-bromo intermediates (compounds **16a–c**) that were dehalogenated and saponified to the desired carboxylic acid analogs (compounds **18a**, **18b**, and **18c**; Figure 2; Tables 1 and S2). The bromo analogs were also hydrolyzed to evaluate the effect of a R^3-bromo substituent in combination with an acetylene spacer in R^1 (compounds **17a**, **17b**, and **17c** in Figure 2; Tables 1 and S2). These analogs were complemented with the brominated compound **20** that lacks the acetylene in position 8 (Figure 2).

In summary, over 100 2-pyridone molecules were synthesized and then screened for their ability to modulate the in vitro aggregation of CsgA into amyloid using the ThT assay. Of the 106 tested compounds, 18 active and three inactive compounds were selected for additional studies (Table 1; **17b**, **17c**, **18c**, and **20** in Figure 2).

Further Characterization of the CsgA Amyloid Inhibitors

The library of compounds was initially tested for modulation of CsgA polymerization using the ThT assay (Figure 3A). To supplement the ThT results, we used additional biophysical assays to assess how the 21 selected compounds were affecting CsgA aggregation. CsgA (5 μM) assembles into large SDS insoluble amyloid polymers after overnight incubation; these aggregates are large enough that they do not migrate into standard SDS gels. Curli inhibitors, including compound **1**, discourage CsgA from adopting an SDS insoluble form, and CsgA runs into the gel after overnight incubation (Figure 3B). SDS solubility after overnight incubation with various compounds (50 μM) corresponded well with the ThT results. Compounds **7**, **8**, **9**, and **10** were potent inhibitors as determined by the ThT and maintained CsgA in an SDS-soluble state (Figures 3A and 3B). Therefore, extension of the peptide backbone in compounds **7** and **8** or introduction of a sultam in compounds **9** and **10** increased the ability of the compound to inhibit CsgA polymerization into amyloid (Table 1; Figures 3A and 3B).

We also probed the aggregation state of CsgA using grafted amyloid-motif antibodies (gammabodies) that recognize CsgA fibrils with conformational and sequence specificity (Ladiwala et al., 2012; Perchiacca et al., 2012). The gammabody used herein contains the amyloidogenic R1 repeating unit domain of CsgA (Wang et al., 2007) grafted into the third complementarity-determining region of a single-domain (V_H) antibody. The CsgA R1 gammabody specifically recognizes polymerized CsgA (Figure 3C). The CsgA samples incubated overnight with compounds found to be inhibitory by ThT analysis also showed reduced gammabody binding (Figure 3C). A control blot detecting all CsgA assured that the results were not due to differences in the amount of deposited CsgA (Figure S1). Moreover, curli fibers were undetectable by transmission electron microscopy (TEM) when CsgA was incubated with inhibitory compounds including compound **7**, one of the most potent inhibitors (Figure 3D and data not shown).

CsgA Amyloid Accelerators

Although most of the compounds we analyzed inhibited or had no affect on CsgA amyloid formation, compounds **17b** and **17c** (brominated intermediates with an acetylene spacer) (Figure 2) were found to accelerate CsgA polymerization into amyloid (Table 1; Figure 4). When compound **17b** or **17c** was incubated with CsgA, the lag phase was reduced in the presence of compounds **17b** or **17c** from 2 hr for the DMSO control to 1 hr with compound **17c** and even shorter with compound **17b** (Figure 4A). Compounds **17b** and **17c** contain a bromine in position 6 and an acetylene spacer in position 8, affording these compounds the unique ability to accelerate CsgA polymerization and promoted the conversion of CsgA into an SDS insoluble form (Figures 1, 3, 4A, and 4B; Table 1). SDS-insoluble CsgA was observed as early as 8 hr when incubated with **17b** or **17c** (Figure 4C). CsgA incubated in the presence of the accelerating compounds was also recognized by the CsgA R1 gammabody, providing additional evidence for amyloid formation (Figure 4D). Notably, the acetylene spacer alone in position 8 (compound **18c**) or bromine in position 6 with an aryl in position 8 (without acetylene spacer, compound **20**) resulted in potent inhibition of curli assembly (Figures 3, 4A, and 4B).

To test the hypothesis that CsgA still assembles into morphologically similar fibers in the presence of compounds **17b** and **17c** in vitro, we examined fibers formed with or without accelerating compounds by TEM. After 6 hr, CsgA formed curli fibers that were loosely assembled in bundles (Figure 4E). CsgA incubated with either of the two accelerating compounds, **17b** or **17c**, for 6 hr also formed abundant large assemblies of fibers that appeared similar to those formed by CsgA (in the absence of such compounds) (Figure 4E). This supports faster assembly of ordered CsgA fibers in the presence of accelerating compounds.

2-Pyridones Modulate Curli-Dependent Biofilm Formation

Small molecules, including D-amino acids and nor-spermidine, can inhibit and disperse pellicle biofilms (Kolodkin-Gal et al., 2010, 2012). The ability of certain 2-pyridones to inhibit CsgA aggregation in vitro inspired us to test the ability of these compounds to block pellicle biofilm formation by *E. coli*. Pellicle biofilms form at the air liquid interface and are dependent on curli fibers (Cegelski et al., 2009; Zhou et al., 2012b). Compound **1** inhibits CsgA amyloid formation in vitro and inhibits pellicle biofilm formation (Figures 2A and 5B; Cegelski et al., 2009). Similarly, compounds **7**, **8**, **18c**, and **20**, which inhibited CsgA fibrillization in vitro, could also inhibit pellicle formation (Figures 2A, 4A, 5A, 5B, and S2A). Interestingly, the accelerating compounds **17b** and **17c** did not appear to affect pellicle formation (Figures 5A and 5B). None of the compounds tested affected growth of the bacteria (Figure S2B).

CsgE Modulates Pellicle Biofilm Formation

Similar to small molecule amyloid inhibitors, molecular chaperones can also inhibit CsgA amyloid formation (Evans et al., 2011). CsgE is a putative periplasmic chaperone and has been shown to prevent CsgA self-assembly into amyloid fibers in vitro (Nenninger et al., 2011) (Figures 6A and 6B). To test whether the interaction between CsgE and CsgA fibers

could prevent further CsgA fiber elongation, we conducted an order of addition experiment where CsgE was added at different times after the start of CsgA polymerization. CsgA was allowed to polymerize for 1, 2, 7, and 8 hr prior to the addition of CsgE. CsgE arrested CsgA polymerization at the time of addition in all cases (Figure 6A). The addition of CsgE to mature CsgA fibers did not disassemble or destabilize fibers (data not shown). These results are consistent with the idea that CsgE prevents fiber elongation, possibly by sequestering soluble CsgA.

We then used surface plasmon resonance to test whether CsgE directly interacts with CsgA amyloid fibers. Purified CsgA was allowed to polymerize for 24 hr. Fibers were then sonicated and immobilized on a GE Sensor-Chip and CsgE was injected over the chip. A rapid increase in resonance units was observed upon addition of CsgE indicating a direct interaction between CsgE and CsgA fibers (Figure 6C, black line). Injection of a mock purification of CsgE to control for possible copurified proteins did not result in a large increase in resonance units (Figure 6C, gray line). CsgE also did not interact with BSA (data not shown). Our SPR experiments using mature CsgA fibers demonstrate that not only can CsgE stabilize CsgA monomers but can also interact with CsgA fibers that may also inhibit monomer addition to fiber ends.

The observation that peptidomimetic compounds could inhibit pellicle biofilms (Figure 5) raised the question of whether proteins naturally found in curli-dependent pellicle biofilms could exert a similar effect. We therefore tested whether exogenous addition of CsgE to pellicle biofilms could inhibit pellicle formation and observed that the addition of purified CsgE could inhibit curli-dependent biofilm formation (Figure 6D).

DISCUSSION

Because amyloid formation is readily associated with human pathologies, research on amyloid modulators has been extensive (Härd and Lendel, 2012; Kim et al., 2010; Ozudogru and Lippa, 2012; Sivanathan and Hochschild, 2012). Utilization of functional amyloid systems to screen for small compounds that affect amyloid formation has proven utility (Horvath et al., 2012; Romero et al., 2013; Sivanathan and Hochschild, 2012). The functional amyloid curli assembled by *E. coli* provides a highly tractable genetic system, straightforward and easily assessable in vivo assays, and good biochemical tools for measuring amyloid formation.

We have used the curli system in *E. coli* to screen for amyloid modulators that are based on the highly amendable 2-pyridone backbone (Cegelski et al., 2009). We found improved inhibitors that are derivatives of compound **1**, which has a well-documented ability to inhibit curli amyloid formation (Figure 1) (Cegelski et al., 2009; Horvath et al., 2012). Improved inhibitors were obtained by extending the peptidomimetic backbone of compound **1** by introducing an amine functionality in the pyridone ring resulting in compound **7** (Horvath et al., 2013; Berg et al., 2006) (Figures 1, 2A, and 2B; Table 1) and the rigidified tricyclic analog (compound **8**; Figures 1, 2A, and 2B; Table 1) (Horvath et al., 2013). The desulfurized ring-opened analog (compound **11**; Figure 1) (Horvath et al., 2013) and analogs that have an oxidized sulfur (sulfoxide—compound **12** or sulfone—compound **13**) lost most

of their inhibitory activity (Figures 3A and 3B; Table 1). Compound **14**, which has both the extended peptidomimetic backbone and oxidized sulfur (Figure 1; Horvath et al., 2013) was able to modestly inhibit CsgA polymerization, showing that the extension of the peptidomimetic backbone is important and can compensate for the loss in activity by the sulfoxide functionality (Figures 2A and 2B; Table 1).

The importance of the carboxylic acid for inhibition of curli formation is clear, as the methyl ester compound **2** did not inhibit CsgA polymerization in vitro or pellicle biofilm formation (Table 1). Variations in this position were thus not further investigated (Horvath et al., 2012). Removing the trifluoro methyl group from compound **1** (to yield compound **3**; Table 1) or introducing a small aromatic group in position 7 (compound **6**; Table 1) reduced the ability to inhibit CsgA polymerization and allowed CsgA to assemble into an SDS-insoluble aggregate (Table 1; Figures 3A and 3B). We could further conclude that by exchanging the five-membered thiazolino group for slightly more flexible six-membered sultams (compounds **9** and **10**; Figure 1) (Sellstedt and Almqvist, 2009), the inhibitory activity was slightly improved (Figures 2A and 2B; Table 1), whereas the corresponding methyl ester compound **5** was inactive and further proved the importance of the carboxylic acid (Figures 3A and 3B; Table 1).

The screening results were also clear regarding the substituent in position 8. By exchanging position 8 from an aryl or hetero aryl for a smaller cyclopropyl substituent the inhibitory effect was completely lost (e.g., **21–31** in Table S1 and **82–84** in Table S2). With this knowledge, we investigated if a spacer between the central fragment and the aryl group in position 8 would impact the activity. Hence, acetylene spacers were introduced via Sonogashira couplings (Figure 2). The introduction of an acetylene unit between the central fragment and the substituent in position 8 resulted in compounds with great inhibitory activity, at least as potent as compound **1**. However, strikingly, two of the synthesis intermediates (compounds **17b** and **17c**) that have bromine at position 6 and an acetylene spacer accelerated CsgA polymerization by reducing the lag phase. These observations suggest that **17b** and **17c** may act either by directing CsgA monomers into an amyloid nucleus or by stabilizing the nucleus conformation. The accelerating compounds did not appear to have an appreciable affect on the elongation rate and CsgA polymerization further supporting a role for **17b** and **17c** primarily during the early oligo-merization stages of amyloid formation. The halide is crucial for the accelerating activity, and future studies will evaluate if other electron-withdrawing groups in the same position can conserve or even enhance this effect. We have previously described how α-synuclein forms on-pathway oligomers faster in the presence of compound **1** (Horvath et al., 2012). It is possible that the accelerating effects observed for compounds **17b** and **17c** on CsgA polymerization follow the same mechanism. However, this is challenging to test because the transition from monomer to fiber is rapid, and oligomers that may have formed are transient and difficult to isolate and characterize.

The discrepancy between inhibitory effect for compounds **9** and **10** in in vitro assays such as the ThT assay and the in vivo pellicle assay may be explained by differences in how the compounds can access the in vivo environment where curli assembly takes place around the

cell. Furthermore, compounds may not work in the in vivo assays because the media used for pellicle growth or the incubation conditions may temper compound activity.

CsgE inhibits CsgA amyloid assembly in vitro and is a putative chaperone inside the bacterial cell, preventing amyloids from forming until CsgA reaches the outside of the cell (Nenninger et al., 2011). Our observations support this mechanism and suggest that CsgE can disrupt on-going fiber formation. Extracellular CsgE-mediated prevention of pellicle biofilm formation suggests that this protein could play a role in the regulation of biofilm development and maturation. Finally, the similarity of effects by adding CsgE or chemical inhibitors to polymerizing CsgA reveals that small molecule inhibitors can mimic the activity of protein chaperones, thus acting as "chemical chaperones."

SIGNIFICANCE

The Earth's microbial population exists predominately in matrix-encased communities called biofilms. Bacterial bio-films present a significant industrial and clinical challenge, and new approaches are needed to combat biofilm formation. The extracellular matrix produced during biofilm growth provides structural rigidity to the community as well as protection from environmental insults. The major proteinaceous components of *E. coli* and other enteric bacterial biofilm matrices are amyloid fibers, called "curli" (McCrate et al., 2013). Environmental biofilms have been discovered to have an abundance of functional amyloids (Larsen et al., 2007). Targeting formation of amyloid fibers could be a means of preventing colonization, invasion, and biofilm formation. 2-Pyridone compounds have been shown previously to possess antiamyloid and antibiofilm activities and this inspired us to further elaborate on the 2-pyri-done scaffold with added functional groups to identify additional antibiofilm compounds. During the characterization of 2-pyridones, we discovered compounds that had both anti-amyloid and proamyloid characteristics. In addition to identifying 2-pyridone molecules with interesting biological activities, we also provide insights into the dynamics of curli-dependent biofilm formation by using both chemical and protein chaperones to prevent in vivo amyloid formation and pellicle biofilm growth. The curli-specific chaperone CsgE was demonstrated to arrest curli aggregation in vitro, and, strikingly, CsgE could also prevent pellicle bio-film formation when added exogenously to cultures. Small organic molecules that target bacterial amyloids and inhibit or disrupt biofilm formation have great potential as new antimicrobial therapeutics. These compounds are potentially valuable tools to dissect the stages of amyloid formation, amyloid inhibition by varying chemical species, and as modulators of amyloid-dependent biofilm formation.

EXPERIMENTAL PROCEDURES

Soluble CsgA Purification

C-terminal His_6-tagged CsgA (Chapman et al., 2002) was, with some modifications, purified as previously described (Cegelski et al., 2009). Briefly, NEB3016 slyD::kan pET11d-sec-csgA-6xhis cells were grown to OD_{600} 0.9, induced with IPTG, and incubated at 37°C for 1 hr. Cells were pelleted by centrifugation and stored at −80°C. Cells were lysed by incubation with stirring in an 8 M guanidine hydrochloride, 50 mM potassium phosphate

solution pH 7.3 for 24 hr at 4°C. The insoluble portion of the lysate was removed by centrifugation and the remaining supernatant was incubated with NiNTA resin (Sigma-Aldrich) for 1 hr at room temperature. The nickel affinity beads were washed with 50 mM potassium phosphate pH 7.3 and a 12.5 mM imidazole, 50 mM potassium phosphate solution. His$_6$-tagged CsgA was eluted with a 125 mM imidazole, 50 mM potassium phosphate solution. Protein concentration was determined by the BCA assay (Thermo Scientific).

CsgE Purification

CsgE-His was, with some modifications, expressed and purified as previously described (Nenninger et al., 2011). Briefly, CsgE-His was expressed from pNH27 (gene encoding cytoplasmic CsgE inserted into the NcoI-BamHI sites of pET11d) in strain NEB 3016 with 100 μg/ml ampicillin. Cells were grown to OD$_{600}$ 0.9 and induced for 1 hr with IPTG. Cells were pelleted by centrifugation and resuspended in lysis buffer. Cells were lysed using a French press and after centrifugation the supernatant was incubated with NiNTA resin (Sigma-Aldrich) at 4°C overnight. The nickel affinity beads were washed with lysis buffer, followed by a 12.5 mM Imidazole, 50 mM potassium phosphate solution pH 7.3. Histagged CsgE was eluted with a 250 mM Imidazole, 50 mM potassium phosphate solution pH 7.3. The protein buffer was exchanged to 50 mM potassium phosphate, 200 mM sodium chloride pH 7.3 with 1 mM PMSF on a Zeba Desalt Spin Column (Thermo Scientific).

In Vitro CsgA Polymerization Inhibition

Compound stock solutions were prepared at 20 mM in DMSO and diluted to appropriate concentrations in 50 mM potassium phosphate buffer pH 7.3. Purified soluble CsgA was diluted to 10 μM in potassium phosphate buffer. Equimolar concentrations of CsgE and CsgA or equal volumes of compound and CsgA were mixed in a 96-well black plate (Corning). Control experiments were performed with 0.5% DMSO. Thioflavin T was added to a final concentration of 20 μM and fluorescence was measured at 480 nm (excitation 440 nm) for 18 hr at 20°C with agitation every 15 min on a Tecan Infinite 200i to monitor amyloid formation.

CsgA Solubility

Freshly purified soluble CsgA and compounds were prepared and monitored for amyloid formation as described above. After 18 hr incubation, 100 μl samples were collected and centrifuged at $16,100 \times g$ for 20 min. The supernatant fractions were transferred to fresh tubes and 30 μl aliquots were mixed with $4 \times$ SDS sample buffer (125 mM Tris pH 6.8, 10% 2-mercaptoethanol, 20% glycerol, 6% sodium dodecyl sulfate, 0.02% bromophenol blue) and incubated at 95°C for 10 min. Samples were loaded on a 15% SDS-PAGE gel and analyzed by PAGE Blue (Fermentas) staining. For the gel presented in Figure 5C, 8 hr samples were not centrifuged and not boiled. In all other aspects, the procedure was the same as described above.

Immunoblotting

Freshly purified soluble CsgA and compounds were prepared and monitored for amyloid formation as described above. After 18 hr incubation, 100 μl samples were collected and centrifuged at $16,100 \times g$ for 30 min. The pellets were resuspended in 200 μl PBS (10 mM PBS) and sonicated for three bursts on ice. Each sample (2.5 μl) was dripped onto a nitrocellulose membrane (Bio-Rad). The membrane was blocked for 2 hr with 10% milk in PBS at room temperature, rinsed with PBS, and thereafter incubated with FLAG-tagged R1 gamma-body at 4°C overnight. After rinsing with PBS, the membrane was incubated with rabbit-anti FLAG antibody, rinsed again with PBS, and incubated with HRP conjugated goat-anti rabbit antibody. Control blots were prepared in the same way, incubated with anti-CsgA antibody produced in rabbit detecting all CsgA as the primary antibody and after washing, incubated with HRP conjugated goat-anti rabbit antibody. Signals were visualized using the Super Signal West Dura Extended Duration Substrate (Thermo Scientific).

TEM and Immunogold

A JEM 1200 transmission electron microscope (Jeol) was used to visualize the CsgA fibers. Samples were placed on formvar-coated nickel grids for 3 min, washed with deionized water two times, and stained with 1% sodium silicotungstate for 1 min. Immunogold experiments were conducted on an MC4100 *csgE* deletion mutant overexpressing CsgE from pTrc99A as described previously (Epstein et al., 2009). The anti-CsgE antibody was diluted 1:5,000 prior to incubation with grids. No primary antibody control grids were incubated with PBS.

Pellicle Biofilm

Appropriate volumes of compound stock solutions in DMSO or purified CsgE were added to 2 ml Luria broth no salt (LBNS) broth in sterile 24-well plates and inoculated with 2 μl of an overnight culture of *E. coli* strain UTI89 grown in Luria broth (LB). The plates were incubated statically at 26°C, and after 48 hr of growth wells were rinsed and stained with crystal violet.

Surface Plasmon Resonance

Interaction studies between CsgA amyloid fibers and CsgE were conducted as previously described with some modification (Zhou et al., 2012a). Forty micro-liters of 1 μM CsgE or an equivalent volume of a mock purification (NEB3013 with pET11d) was injected over the sensor chip at 20 μl/min. The injection was stopped at 120 s, and the flow of 50 mM potassium phosphate, 200 mM sodium chloride buffer was resumed. The response was recorded in resonance units.

Organic Compounds

Compound synthesis and characterization is described in the Supplemental Experimental Procedures.

Supplementary Material

Refer to Web version on PubMed Central for supplementary material.

Acknowledgments

References

Andersson EK, Chapman M. Small molecule disruption of *B. subtilis* biofilms by targeting the amyloid matrix. Chem Biol. 2013; 20:5–7. [PubMed: 23352134]

Ban T, Hamada D, Hasegawa K, Naiki H, Goto Y. Direct observation of amyloid fibril growth monitored by thioflavin T fluorescence. J Biol Chem. 2003; 278:16462–16465. [PubMed: 12646572]

Barnhart MM, Chapman MR. Curli biogenesis and function. Annu Rev Microbiol. 2006; 60:131–147. [PubMed: 16704339]

Berg V, Sellstedt M, Hedenström M, Pinkner JS, Hultgren SJ, Almqvist F. Design, synthesis and evaluation of peptidomimetics based on substituted bicyclic 2-pyridones-targeting virulence of uropathogenic *E. coli*. Bioorg Med Chem. 2006; 14:7563–7581. [PubMed: 16904898]

Bian Z, Normark S. Nucleator function of CsgB for the assembly of adhesive surface organelles in *Escherichia coli*. EMBO J. 1997; 16:5827–5836. [PubMed: 9312041]

Blanco LP, Evans ML, Smith DR, Badtke MP, Chapman MR. Diversity, biogenesis and function of microbial amyloids. Trends Microbiol. 2012; 20:66–73. [PubMed: 22197327]

Cegelski L, Pinkner JS, Hammer ND, Cusumano CK, Hung CS, Chorell E, Aberg V, Walker JN, Seed PC, Almqvist F, et al. Small-molecule inhibitors target *Escherichia coli* amyloid biogenesis and bio-film formation. Nat Chem Biol. 2009; 5:913–919. [PubMed: 19915538]

Chapman MR, Robinson LS, Pinkner JS, Roth R, Heuser J, Hammar M, Normark S, Hultgren SJ. Role of *Escherichia coli* curli operons in directing amyloid fiber formation. Science. 2002; 295:851–855. [PubMed: 11823641]

Chiti F, Dobson CM. Protein misfolding, functional amyloid, and human disease. Annu Rev Biochem. 2006; 75:333–366. [PubMed: 16756495]

Chorell E, Pinkner JS, Bengtsson C, Edvinsson S, Cusumano CK, Rosenbaum E, Johansson LBÅ, Hultgren SJ, Almqvist F. Design and synthesis of fluorescent pilicides and curlicides: bioactive tools to study bacterial virulence mechanisms. Chemistry. 2012; 18:4522–4532. [PubMed: 22431310]

DePas WH, Hufnagel DA, Lee JS, Blanco LP, Bernstein HC, Fisher ST, James GA, Stewart PS, Chapman MR. Iron induces bimodal population development by *Escherichia coli*. Proc Natl Acad Sci USA. 2013; 110:2629–2634. [PubMed: 23359678]

Epstein EA, Reizian MA, Chapman MR. Spatial clustering of the curlin secretion lipoprotein requires curli fiber assembly. J Bacteriol. 2009; 191:608–615. [PubMed: 19011034]

Evans ML, Schmidt JC, Ilbert M, Doyle SM, Quan S, Bardwell JC, Jakob U, Wickner S, Chapman MR. *E. coli* chaperones DnaK, Hsp33 and Spy inhibit bacterial functional amyloid assembly. Prion. 2011; 5:323–334. [PubMed: 22156728]

Fowler DM, Koulov AV, Alory-Jost C, Marks MS, Balch WE, Kelly JW. Functional amyloid formation within mammalian tissue. PLoS Biol. 2006; 4:e6. [PubMed: 16300414]

Hammar M, Arnqvist A, Bian Z, Olsén A, Normark S. Expression of two CSG operons is required for production of fibronectin-and congo red-binding curli polymers in *Escherichia coli K-12*. Mol Microbiol. 1995; 18:661–670. [PubMed: 8817489]

Hammar M, Bian Z, Normark S. Nucleator-dependent intercellular assembly of adhesive curli organelles in *Escherichia coli*. Proc Natl Acad Sci USA. 1996; 93:6562–6566. [PubMed: 8692856]

Hammer ND, Schmidt JC, Chapman MR. The curli nucleator protein, CsgB, contains an amyloidogenic domain that directs CsgA polymerization. Proc Natl Acad Sci USA. 2007; 104:12494–12499. [PubMed: 17636121]

Hammer ND, Wang X, McGuffie BA, Chapman MR. Amyloids: friend or foe? J Alzheimers Dis. 2008; 13:407–419. [PubMed: 18487849]

Horvath I, Weise CF, Andersson EK, Chorell E, Sellstedt M, Bengtsson C, Olofsson A, Hultgren SJ, Chapman M, Wolf-Watz M, et al. Mechanisms of protein oligomerization: inhibitor of functional amyloids templates α-synuclein fibrillation. J Am Chem Soc. 2012; 134:3439–3444. [PubMed: 22260746]

Horvath I, Sellstedt M, Weise C, Nordvall LM, Krishna Prasad G, Olofsson A, Larsson G, Almqvist F, Wittung-Stafshede P. Modulation of α-synuclein fibrillization by ring-fused 2-pyridones: templation and inhibition involve oligomers with different structure. Arch Biochem Biophys. 2013; 532:84–90. [PubMed: 23399432]

Härd T, Lendel C. Inhibition of amyloid formation. J Mol Biol. 2012; 421:441–465. [PubMed: 22244855]

Kim J, Kobayashi M, Fukuda M, Ogasawara D, Kobayashi N, Han S, Nakamura C, Inada M, Miyaura C, Ikebukuro K, Sode K. Pyrroloquinoline quinone inhibits the fibrillation of amyloid proteins. Prion. 2010; 4:26–31. [PubMed: 20083898]

Kolodkin-Gal I, Romero D, Cao S, Clardy J, Kolter R, Losick R. D-amino acids trigger biofilm disassembly. Science. 2010; 328:627–629. [PubMed: 20431016]

Kolodkin-Gal I, Cao S, Chai L, Böttcher T, Kolter R, Clardy J, Losick R. A self-produced trigger for biofilm disassembly that targets exopolysaccharide. Cell. 2012; 149:684–692. [PubMed: 22541437]

Ladiwala AR, Bhattacharya M, Perchiacca JM, Cao P, Raleigh DP, Abedini A, Schmidt AM, Varkey J, Langen R, Tessier PM. Rational design of potent domain antibody inhibitors of amyloid fibril assembly. Proc Natl Acad Sci USA. 2012; 109:19965–19970. [PubMed: 23161913]

Larsen P, Nielsen JL, Dueholm MS, Wetzel R, Otzen D, Nielsen PH. Amyloid adhesins are abundant in natural biofilms. Environ Microbiol. 2007; 9:3077–3090. [PubMed: 17991035]

Loferer H, Hammar M, Normark S. Availability of the fibre subunit CsgA and the nucleator protein CsgB during assembly of fibronectin-binding curli is limited by the intracellular concentration of the novel lipoprotein CsgG. Mol Microbiol. 1997; 26:11–23. [PubMed: 9383186]

McCrate, OA.; Zhou, X.; Reichhardt, C.; Cegelski, L. Sum of the parts: composition and architecture of the bacterial extracellular matrix. J Mol Biol. 2013. Published online July 1, 2013 http://dx.doi.org/10.1016/j.jmb.2013.06.022

Naiki H, Higuchi K, Hosokawa M, Takeda T. Fluorometric determination of amyloid fibrils in vitro using the fluorescent dye, thioflavin T1. Anal Biochem. 1989; 177:244–249. [PubMed: 2729542]

Nenninger AA, Robinson LS, Hultgren SJ. Localized and efficient curli nucleation requires the chaperone-like amyloid assembly protein CsgF. Proc Natl Acad Sci USA. 2009; 106:900–905. [PubMed: 19131513]

Nenninger AA, Robinson LS, Hammer ND, Epstein EA, Badtke MP, Hultgren SJ, Chapman MR. CsgE is a curli secretion specificity factor that prevents amyloid fibre aggregation. Mol Microbiol. 2011; 81:486–499. [PubMed: 21645131]

Ozudogru SN, Lippa CF. Disease modifying drugs targeting β-amyloid. Am J Alzheimers Dis Other Demen. 2012; 27:296–300. [PubMed: 22815077]

Perchiacca JM, Ladiwala ARA, Bhattacharya M, Tessier PM. Structure-based design of conformation- and sequence-specific antibodies against amyloid β. Proc Natl Acad Sci USA. 2012; 109:84–89. [PubMed: 22171009]

Robinson LS, Ashman EM, Hultgren SJ, Chapman MR. Secretion of curli fibre subunits is mediated by the outer membrane-localized CsgG protein. Mol Microbiol. 2006; 59:870–881. [PubMed: 16420357]

Romero D, Sanabria-Valentín E, Vlamakis H, Kolter R. Biofilm inhibitors that target amyloid proteins. Chem Biol. 2013; 20:102–110. [PubMed: 23352144]

Römling U. Characterization of the rdar morphotype, a multicellular behaviour in Enterobacteriaceae. Cell Mol Life Sci. 2005; 62:1234–1246. [PubMed: 15818467]

Sellstedt M, Almqvist F. Synthesis of a novel tricyclic peptidomimetic scaffold. Org Lett. 2008; 10:4005–4007. [PubMed: 18702499]

Sellstedt M, Almqvist F. A novel heterocyclic scaffold formed by ring expansion of a cyclic sulfone to sulfonamides. Org Lett. 2009; 11:5470–5472. [PubMed: 19891461]

Shewmaker F, McGlinchey RP, Thurber KR, McPhie P, Dyda F, Tycko R, Wickner RB. The functional curli amyloid is not based on in-register parallel beta-sheet structure. J Biol Chem. 2009; 284:25065–25076. [PubMed: 19574225]

Shu Q, Crick SL, Pinkner JS, Ford B, Hultgren SJ, Frieden C. The *E. coli* CsgB nucleator of curli assembles to β-sheet oligomers that alter the CsgA fibrillization mechanism. Proc Natl Acad Sci USA. 2012; 109:6502–6507. [PubMed: 22493266]

Sivanathan V, Hochschild A. Generating extracellular amyloid aggregates using *E. coli* cells. Genes Dev. 2012; 26:2659–2667. [PubMed: 23166018]

Taylor JD, Zhou YZ, Salgado PS, Patwardhan A, McGuffie M, Pape T, Grabe G, Ashman E, Constable SC, Simpson PJ, et al. Atomic resolution insights into curli fiber biogenesis. Structure. 2011; 19:1307–1316. [PubMed: 21893289]

Wang X, Smith DR, Jones JW, Chapman MR. In vitro polymerization of a functional *Escherichia coli* amyloid protein. J Biol Chem. 2007; 282:3713–3719. [PubMed: 17164238]

Wang X, Hammer ND, Chapman MR. The molecular basis of functional bacterial amyloid polymerization and nucleation. J Biol Chem. 2008; 283:21530–21539. [PubMed: 18508760]

Wang X, Zhou YZ, Ren JJ, Hammer ND, Chapman MR. Gatekeeper residues in the major curlin subunit modulate bacterial amyloid fiber biogenesis. Proc Natl Acad Sci USA. 2010; 107:163–168. [PubMed: 19966296]

White AP, Gibson DL, Kim W, Kay WW, Surette MG. Thin aggregative fimbriae and cellulose enhance long-term survival and persistence of *Salmonella*. J Bacteriol. 2006; 188:3219–3227. [PubMed: 16621814]

Zhou Y, Blanco LP, Smith DR, Chapman MR. Bacterial amyloids. Methods Mol Biol. 2012a; 849:303–320. [PubMed: 22528099]

Zhou Y, Smith D, Leong BJ, Brännström K, Almqvist F, Chapman MR. Promiscuous cross-seeding between bacterial amyloids promotes interspecies biofilms. J Biol Chem. 2012b; 287:35092–35103. [PubMed: 22891247]
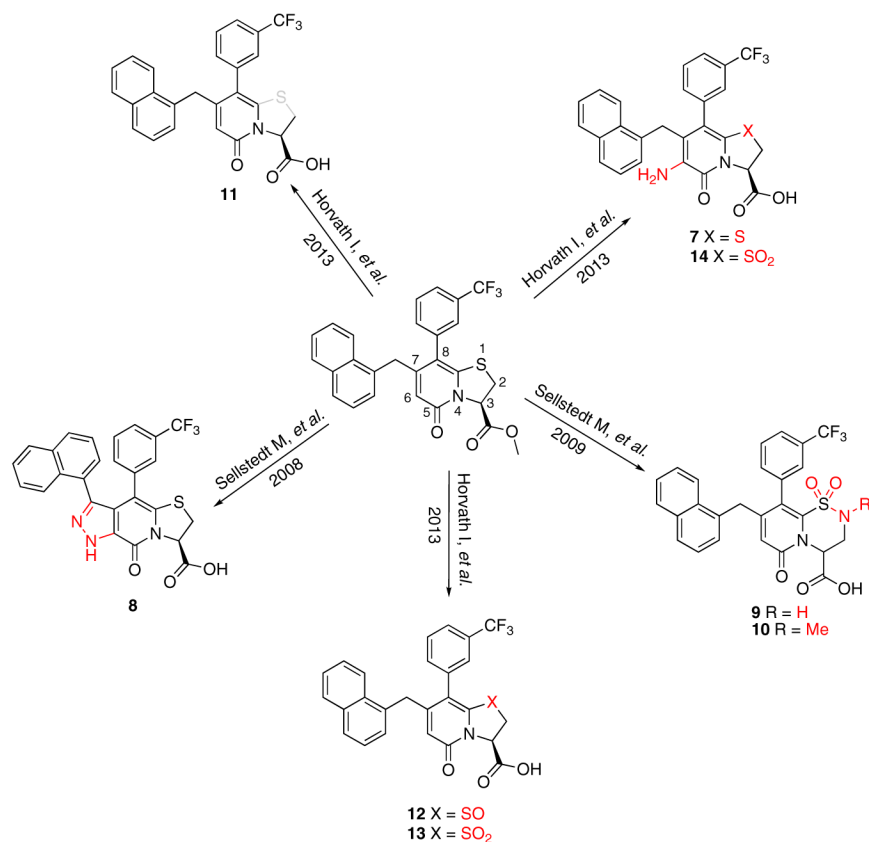
Figure 1. Compounds Synthesized to Analyze Central Fragment Alterations and Substituents
With **1** as starting point, the peptidomimetic backbone was extended by introducing an amine in the pyridone ring resulting in compound **7**. A rigidified tricyclic structure, compound **8**, was included as well as analogs where the five-membered thiazolino group had been exchanged for six-membered sultams in compounds **9** and **10**. Compound **11** is a desulfurized ring-opened analog and compounds **12** and **13** are analogs where the sulfur had been oxidized to the corresponding sulfoxide or sulfone. Compound **14** has both the extended peptidomimetic backbone and oxidized sulfur.
See also Table S1.
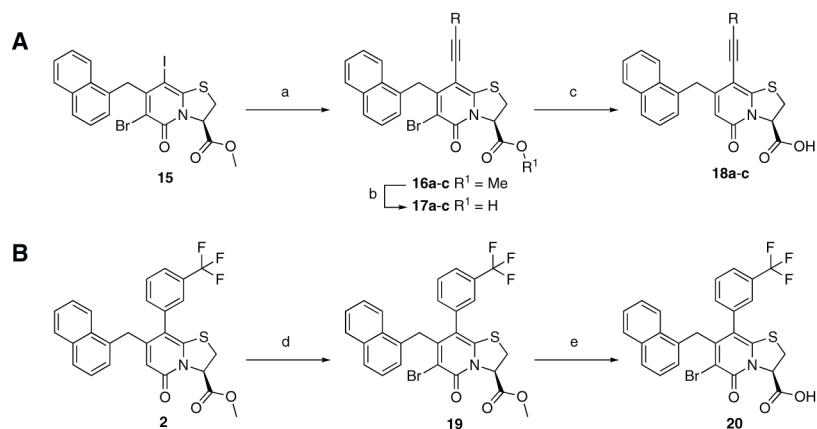
Conditions a) Pd(PPh₃)₂Cl₂, alkyne, CuI, TEA, DMF, rt or 50 °C b) LiOH in THF at rt or LiI in pyridine MWI 130 °C for 15 min c) Zn(s), AcOH, 100 °C d) NBS, MeCN, rt, 91% e) 1M LiOH, THF, rt, 89%.

Entry	R	Compound (yield %)	Compound (yield %)	Compound (yield %)
1	*c*Pr	**16a** (82)	**17a** (63)	**18a** (75)
2	Ph	**16b** (82)	**17b** (67)	**18b** (83)
3	*m*CF₃Ph	**16c** (91)[a]	**17c** (75)[b]	**18c** (63)

[a]Reaction was performed at 50 °C , [b]LiI in pyridine, MWI 130 °C for 15 min was used.

Figure 2. Synthesis of the Acetylene Spacer Analogs and the Brominated Analog of 1

(A) Synthesis of acetylene spacer analogs **18a**, **18b**, and **18c**. The intermediates **17a**, **17b**, and **17c**, with bromine (Br) residues at position 6 were also hydrolyzed and tested for biological activity.

(B) Bromination of **1** to obtain compound **20**.

See also Table S2.
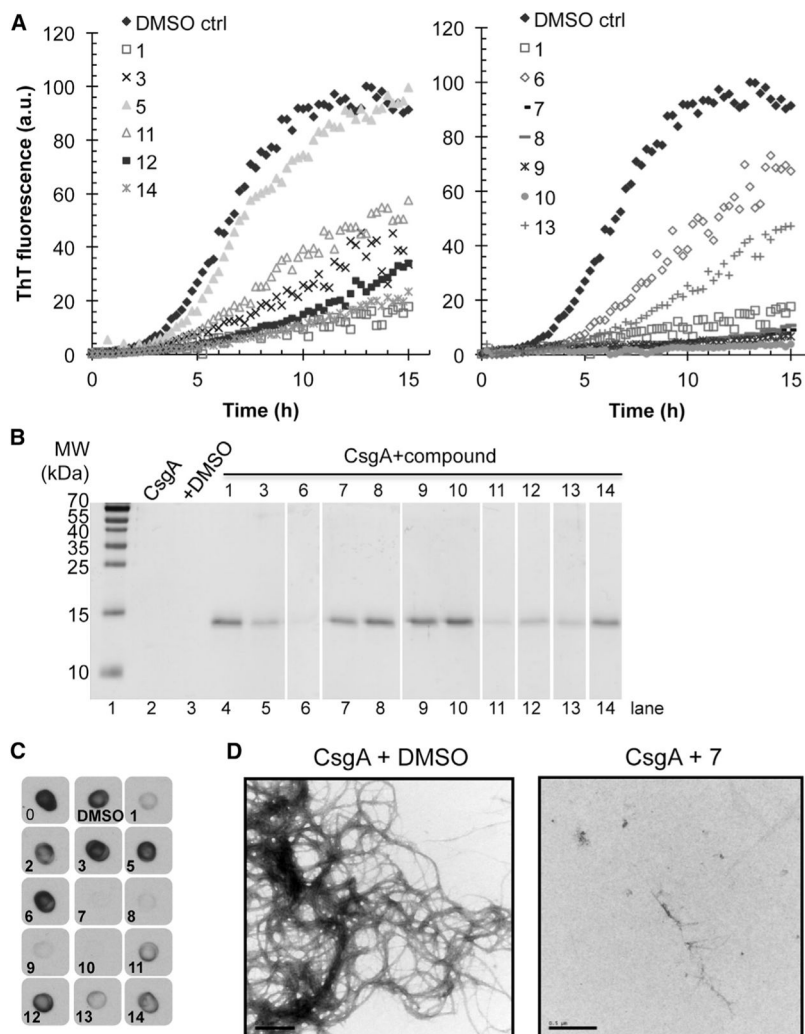
Figure 3. In Vitro Effect of Inhibitory Compounds on CsgA Polymerization

(A) ThT fluorescence of freshly purified 5 μM CsgA with or without 50 μM compound. Reduction in ThT fluorescence corresponds to inhibition of CsgA polymerization.

(B) CsgA solubility after overnight incubation with or without compound by SDS-PAGE. Compounds that inhibit CsgA polymerization kept CsgA in a soluble SDS-sensitive state.

(C) CsgA incubated overnight with compounds was spotted onto a nitrocellulose membrane and probed with a gammabody grafted with the CsgA R1 sequence that detects CsgA amyloid structure.

(D) Transmission electron microscopy of freshly purified CsgA incubated for 6 hr revealed abundant fibers, whereas no curli fibers were detected by when freshly purified CsgA was incubated for 6 hr with the inhibitor compound **7**. Scale bars represent 0.5 μM.

See also Figure S1.
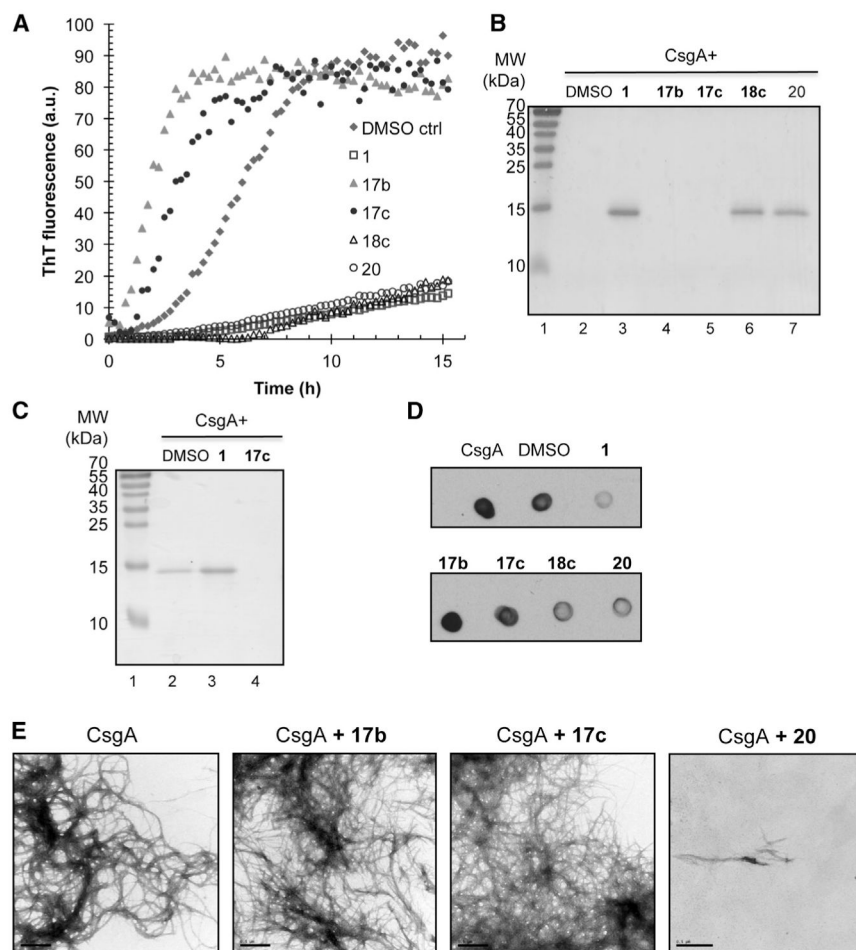
Figure 4. In Vitro Effect of Accelerating Compounds on CsgA Polymerization
(A) ThT fluorescence of freshly purified 5 μM CsgA with or without 50 μM compound. The lag phase of the fluorescence curve as a consequence of ThT binding to polymerizing CsgA was shortened when accelerating compounds **17b** and **17c** were present.
(B) SDS-PAGE of CsgA incubated overnight with or without compound. No soluble CsgA was detected after incubation with accelerators **17b** and **17c** (lanes 4 and 5, respectively).
(C) SDS-PAGE of CsgA incubated for 8h with or without compound. Incubation with the accelerating compound **17c** results in a SDS-insoluble amyloid after 8 hr (lane 4) whereas pure CsgA is still partly soluble (lane 2). In the presence of the inhibitory compound **1**, CsgA is soluble (lane 3).
(D) CsgA incubated overnight with compounds was spotted onto a nitrocellulose membrane and probed with the Tessier gammabody grafted with the CsgA R1 sequence that detects CsgA amyloid structure.
(E) Transmission electron microscopy of CsgA. Negative staining of freshly purified CsgA incubated for 6 hr (left). Freshly purified CsgA incubated for 6h with accelerators **17b** or **17c** appeared similar to CsgA alone. Fibers were not detectable when CsgA was incubation with the chemically similar, yet functionally inhibitory, compound **20**. Scale bars represent 0.5 μM.

See also Figure S1.
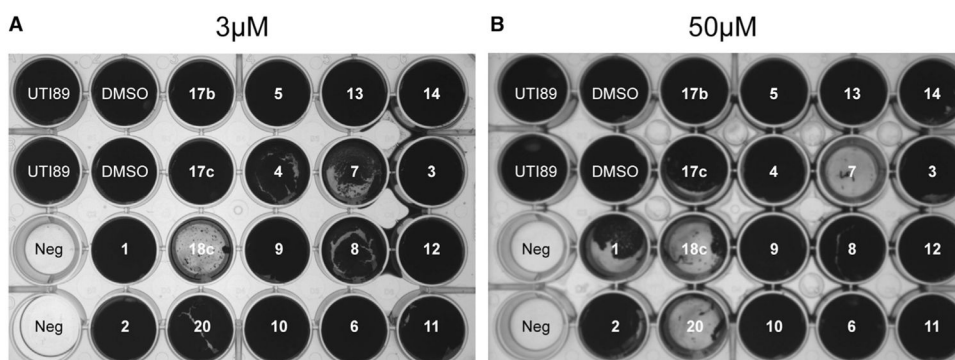
Figure 5. Inhibition of Pellicle Biofilm by Chemical Compounds

(A) Effect of the compounds at a concentration of 3 μM on the formation of curli-dependent pellicle biofilm, incubated at 26°C for 48 hr. Compound **18c** was the most potent inhibitor.

(B) Effect of the compounds at a concentration of 50 μM on the formation of curli-dependent pellicle biofilm, incubated at 26°C for 48 hr. Compounds **7**, **18c**, and **20** were correspondingly efficient in vitro.

See also Figure S2.
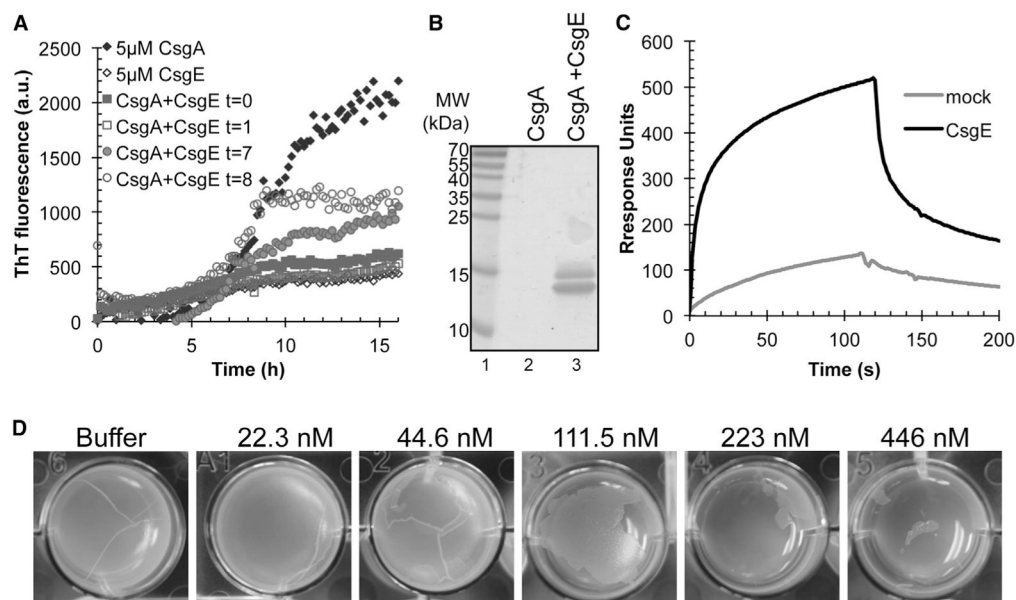
Figure 6. Effect of CsgE on CsgA Polymerization and Pellicle Formation

(A) Immuno-gold labeling of overexpressed CsgE. MC4100 *csgE* mutant cells with empty vector (left) or overexpressing CsgE (middle and right) were incubated with CsgE antibody (left and middle) or buffer (right) followed by incubation with gold particle conjugated secondary antibody prior to uranyl acetate staining and TEM. Scale bar represents 200 nm.
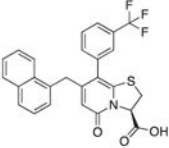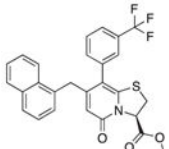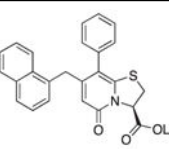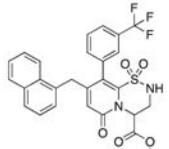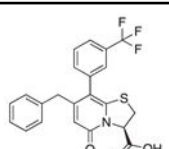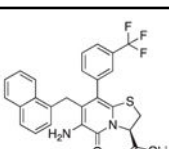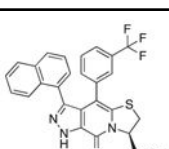
(B) CsgE interacts with CsgA fibers. Surface plasmon resonance sensograms of 1 μM purified CsgE (solid line) or a mock purification (dotted line) were injected over immobilized sonicated CsgA fibers on a CM5 sensor chip. Flow of phosphate buffer was resumed after 120 s.
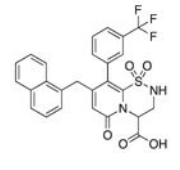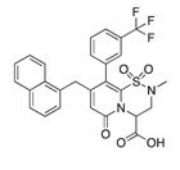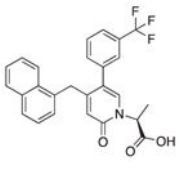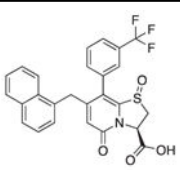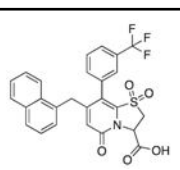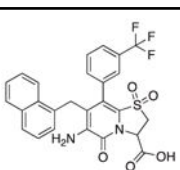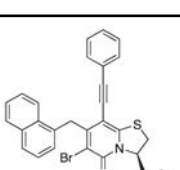
(C) CsgE added to freshly purified CsgA or CsgA incubated for 1 hr inhibits CsgA polymerization. CsgE added to CsgA incubated for 7 hr or 8 hr efficiently inhibits further polymerization.
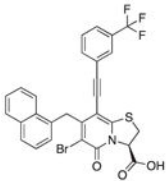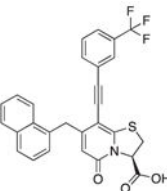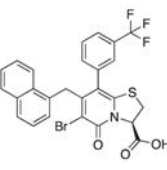
(D) SDS-PAGE after CsgA overnight incubation with or without equimolar concentration of the chaperone CsgE. No CsgA is left in solution when incubated alone (lane 2) whereas CsgA incubated with CsgE (lane 3) was still in a soluble form.

(E) Extracellular addition of CsgE prevents formation of curli-dependent pellicle biofilm in a concentration-dependent manner.

Table 1

Percent ThT Fluorescence Inhibition after Overnight Incubation at 50 μM Compound and 5 μM CsgA

ID	Structure	Mean Inhibition (%)	Maximum (%)	Minimum (%)
1		89	95	72
2		4	16	0
3		57	89	11
5		5	12	0
6		21	25	6
7		90	98	84
8		88	92	74

ID	Structure	Mean Inhibition (%)	Maximum (%)	Minimum (%)
9		92	97	89
10		96	97	87
11		44	80	19
12		64	71	37
13		48	80	22
14		78	85	75
17b		*a*		

ID	Structure	Mean Inhibition (%)	Maximum (%)	Minimum (%)
17c		*a*		
18c		81	89	57
20		80	87	67

Based on four individual experiments. See also Table S1.

[a]Promoting amyloid formation, shorter lag phase.